Conference Proceedings of the Society for Experimental Mechanics Series

H. Jerry Qi · Bonnie Antoun · Richard Hall · Hongbing Lu
Alex Arzoumanidis · Meredith Silberstein · Jevan Furmanski
Alireza Amirkhizi · Joamin Gonzalez-Gutierrez *Editors*

Challenges in Mechanics of Time-Dependent Materials, Volume 2

Proceedings of the 2014 Annual Conference on Experimental and Applied Mechanics

SEM

Springer

Conference Proceedings of the Society for Experimental Mechanics Series

Series Editor
Tom Proulx
Society for Experimental Mechanics, Inc.
Bethel, CT, USA

For further volumes:
http://www.springer.com/series/8922

H. Jerry Qi • Bonnie Antoun • Richard Hall • Hongbing Lu
Alex Arzoumanidis • Meredith Silberstein • Jevan Furmanski
Alireza Amirkhizi • Joamin Gonzalez-Gutierrez
Editors

Challenges in Mechanics of Time-Dependent Materials, Volume 2

Proceedings of the 2014 Annual Conference on Experimental and Applied Mechanics

Springer

Editors
H. Jerry Qi
Georgia Institute of Technology
Atlanta, GA, USA

Richard Hall
Air Force Research Laboratory
Wright-Patterson AFB, OH, USA

Alex Arzoumanidis
Psylotech, Inc.
Evanston, IL, USA

Jevan Furmanski
ExxonMobil
Los Alamos, NM, USA

Joamin Gonzalez-Gutierrez
University of Ljubljana
Ljubljana, Slovenia

Bonnie Antoun
Sandia National Laboratories
Livermore, CA, USA

Hongbing Lu
The Erik Johnson School of Engineering, EC-38
University of Texas-Dallas
Dallas, TX, USA

Meredith Silberstein
Cornell University
Ithaca, NY, USA

Alireza Amirkhizi
University of California
San Diego, La Jolla, CA, USA

ISSN 2191-5644 ISSN 2191-5652 (electronic)
ISBN 978-3-319-06979-1 ISBN 978-3-319-06980-7 (ebook)
DOI 10.1007/978-3-319-06980-7
Springer Cham Heidelberg New York Dordrecht London

Library of Congress Control Number: 2012952717

Printed on acid-free paper

Springer is part of Springer Science+Business Media (www.springer.com)

Preface

Challenges in Mechanics of Time-Dependent Materials, Volume 2: Proceedings of the 2014 Annual Conference on Experimental and Applied Mechanics represents one of the eight volumes of technical papers presented at the SEM 2013 SEM Annual Conference & Exposition on Experimental and Applied Mechanics, organized by the Society for Experimental Mechanics and held in Greenville, SC, June 2–5, 2014. The complete proceedings also include volumes on: *Dynamic Behavior of Materials; Advancement of Optical Methods in Experimental Mechanics; Mechanics of Biological Systems and Materials; MEMS and Nanotechnology; Composite, Hybrid, and Multifunctional Materials; Fracture, Fatigue, Failure and Damage Evolution; and Experimental and Applied Mechanics*.

Each collection presents early findings from experimental and computational investigations on an important area within Experimental Mechanics, the Mechanics of Time-Dependent Materials being one of these areas.

This track was organized to address constitutive, time (or rate)-dependent constitutive, and fracture/failure behavior of a broad range of materials systems, including prominent research in both experimental and applied mechanics. Papers concentrating on both modeling and experimental aspects of Time-Dependent Materials are included.

The track organizers thank the presenters, authors, and session chairs for their participation and contribution to this track. The support and assistance from the SEM staff is also greatly appreciated.

Atlanta, GA, USA — H. Jerry Qi
Livermore, CA, USA — Bonnie Antoun
Wright-Patterson AFB, OH, USA — Richard Hall
Dallas, TX, USA — Hongbing Lu
Evanston, IL, USA — Alex Arzoumanidis
Ithaca, NY, USA — Meredith Silberstein
Los Alamos, NM, USA — Jevan Furmanski
San Diego, La Jolla, CA, USA — Alireza Amirkhizi
Ljubljana, Slovenia — Joamin Gonzalez-Gutierrez

Contents

Chapter 1
Unimorph Shape Memory Polymer Actuators Incorporating Transverse Curvature in the Substrate

Jason T. Cantrell and Peter G. Ifju

Abstract Shape memory polymers (SMP) utilized in reconfigurable structures have the potential to be used in a variety of settings. This paper is primarily concerned with the use of Veriflex-S shape memory polymer and bi-directional carbon fiber in a unimorph actuator configuration. One of the major deficiencies of SMP unimorphs is the permanent set (unrecovered shape) after a single or multiple temperature cycle(s). The novel concept of incorporating transverse curvature in the composite substrate, similar to that of an extendable tape measurer, was proposed to improve the shape recovery. A set of experiments was designed to investigate the influence of transverse curvature, the relative widths of SMP and composite substrates, and shape memory polymer thickness on actuator recoverability after multiple thermomechanical cycles. Flat carbon fiber and shape memory polymer unimorph actuators were evaluated for performance versus actuators of increasing transverse curvature. Digital image correlation was implemented to quantify the out-of-plane deflection of the unimorph composite actuators (UCAs) during the actuation cycle. Experimental results indicate that an actuator with transverse curvature significantly reduces the residual deformation while increasing the shape memory recoverability which could be further tailored to enhance the performance of shape memory polymers in reconfigurable arrangements.

Keywords Shape memory polymer • Unimorph • Transverse curvature • Digital image correlation • Composite

Nomenclature

CF	Carbon fiber
DIC	Digital image correlation
MAV	Micro air vehicle
SMP	Shape memory polymer
T_g	Glass transition temperature
u, v, w	Lengthwise widthwise, and vertical displacements
UCA	Unimorph composite actuator
VIC	Visual image correlation
x, y, z	Lengthwise widthwise, and vertical coordinates

1.1 Introduction

Shape memory polymers (SMPs) are a category of smart material with the ability to change their shape upon the application of external stimuli such as temperature electricity, magnetism, or light. Classes of smart materials include piezoelectric, shape memory alloys, and shape memory polymers. Varieties of smart materials practical for various applications include shape memory alloys in orthodontic treatments, piezoelectric actuators for control of micro air vehicles, shape memory

J.T. Cantrell (✉) • P.G. Ifju
Mechanical and Aerospace Engineering Department, University of Florida, MAE Receiving, 134 MAE-C, Gainesville, FL 32611, USA
e-mail: jasontcantrell@gmail.com; ifju@ufl.edu

H.J. Qi et al. (eds.), *Challenges in Mechanics of Time-Dependent Materials, Volume 2: Proceedings of the 2014 Annual Conference on Experimental and Applied Mechanics*, Conference Proceedings of the Society for Experimental Mechanics Series,
DOI 10.1007/978-3-319-06980-7_1,

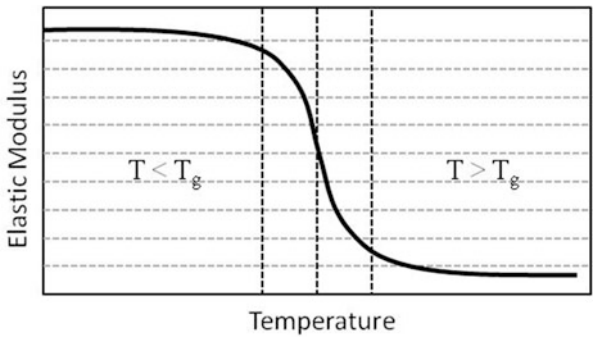

Fig. 1.1 Generalized plot of the elastic modulus (E) versus temperature for Veriflex SMP. The graph is divided into the plastic ($T < T_g$), transition, and rubbery ($T > T_g$) regions

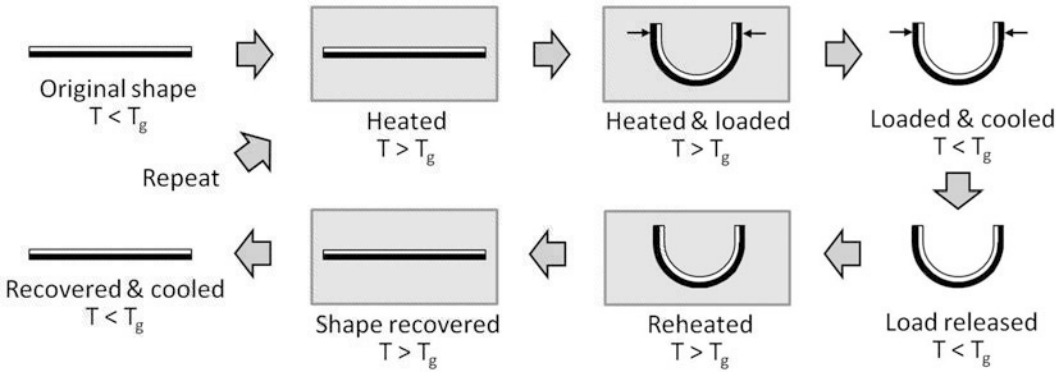

Fig. 1.2 Illustration of a shape memory cycle for recovery of thermally activated SMPs

polymers as cardiovascular stents, and a multitude of smart materials for the morphing of aircraft structures [1–5]. Veriflex-S, the SMP used during the studies in this paper, uses a thermal external stimulus to allow reconfiguration and recovery. This material's properties, and those of its higher temperature counterpart, Veriflex-E, have been studied extensively by researchers including Fulcher et al. [6–8], Nahid et al. [9], McClung et al. [10–14], Liu et al. [15], and Atli et al. [16]. The Veriflex SMPs have been utilized for notable applications including active disassembly for recycling, deployment of satellite solar panels, and deployable aircraft wings [17–19].

Veriflex can be divided into two categories of stiffness and material behavior: the high glassy modulus and low rubbery modulus [12, 13]. At temperatures below their glass transition temperature (T_g), the material is relatively stiff and has a high elastic modulus; however once the SMP is heated above T_g the modulus drops by several orders of magnitude. This transition from the glassy to the rubbery state is illustrated in Fig. 1.1. In the rubbery state, shape memory polymers can deform at levels up to 400 % and after cooling below T_g maintain this new shape indefinitely [20]. The original shape can be recovered by heating the polymer above T_g again. The glassy state is classified as the temperatures lying 10 °C or more below the T_g, while the rubbery state is identified as temperatures lying 10 °C or greater above the T_g [21]. The area in between the glassy and rubbery state is classified as the transition region in which the elastic modulus transitions rapidly.

SMPs can change their shape from their original cast shape (flat beams in this study) to a deformed shape and return to the original shape when exposed to elevated temperatures. An illustration of an ideal shape memory thermomechanical cycle is shown in Fig. 1.2. The SMP begins in its original shape at a high modulus below T_g and then heat is applied to the sample causing the modulus to fall into the rubbery state. Once in the rubbery state the sample is bent into the desired deformed shape (a U-shaped configuration for this study) and then allowed to cool below T_g locking the current deformed shape. The sample can be stored at this configuration to await the reapplication of heat. After heating the sample will release and return to the unconstrained original form. The sample is then cooled and would ideally return to 100 % of the original shape seen before the heating cycle. However, in reality, the Veriflex SMP can achieve a final shape that is only close to the original shape. Various researchers have studied this behavior and determined that the recoverability of SMP can vary between 65 and 95 % of the original shape after repeated cycling depending upon testing conditions [12, 18, 22, 23].

Despite these hindrances SMPs are still advantageous over other shape memory materials due to the fact that they are low cost low density, and highly deformable among other benefits [24, 25]. Shape memory materials are valued for their potential use in adaptive structures in applications such as micro air vehicles (MAVs) and morphing aircraft [26]. The University of Florida has worked with adaptive structures and MAVs extensively, adopting both active adaptation

with piezoelectric actuators and passive adaptation with flexible membrane wings [2, 3, 27–31]. Ifju et al. developed a bendable load stiffened MAV wing that is compliant in the downward direction for storing the aircraft, but uses the wing curvature to avoid buckling due to flight loads [32]. Using this knowledge of MAVs and morphing wing structures, a plan of study was devised for a multipurpose morphing actuator to determine if the same bendable composite technology used in MAV wings could assist in increasing the recoverability of the Veriflex-S SMP. In order to properly understand the overall performance of the SMP in a unimorph composite actuator (UCA) configuration, extensive digital image correlation (DIC) testing was required to determine the residual deformation present. A UCA was described as an element capable of bi-stable configuration when supplied with an external stimulus consisting of one active layer (SMP) to which the stimulus is applied and one inactive layer (carbon fiber laminate) that supports the active layer. A simple flat carbon fiber (CF) beam with SMP adhered to its surface was compared against a transversely curved CF beam with curvature similar to that of the MAV wing discussed previously. Additionally, a more detailed survey investigating the influence of other variables present was also documented via DIC. The details of the UCA analysis and the experimental procedure are explained in the subsequent sections. During the course of experimenting with flat generic unimorph actuators, research indicated that by incorporating a transverse curvature (similar to an extendable tape measure) in the composite layer one can vastly improve the shape recovery of an SMP unimorph actuator. The following paper will cover the findings from the investigation of generic SMP unimorphs.

1.2 Unimorph Composite Actuator Experimental Procedure

1.2.1 Unimorph Composite Actuator (UCA) Fabrication

Each unimorph composite actuator consists of a layer of SMP bonded to a graphite/epoxy substrate. Both flat carbon fiber composite unimorphs and unimorphs incorporating transverse curvature followed the same fabrication methodology. A single layer of [$\pm 45^{\circ}$] oriented plain weave, bi-directional carbon fiber was cut and placed on a Teflon covered plate or curved tooling board. The entire assembly was covered in an additional layer of Teflon, vacuum bagged, and cured at 130 °C for 4 h. After curing, the carbon fiber was cut down to the appropriate size, then a Veriflex-S shape memory polymer panel was bonded to it using Araldite 2011 two-part epoxy. After the epoxy cured the actuators were coated with a base coat of flat white spray paint then speckled for DIC using flat black spray paint.

1.2.2 Digital Image Correlation (DIC) Set-Up

The primary objective of this research was to determine the deformation and shape of the composite beam samples. This was done through the use of the DIC system a non-contact, full-field shape and deformation technique developed at the University of South Carolina [33, 34]. The system uses two Point Grey Research 5-megapixel grayscale cameras to simultaneously capture images of the random speckle pattern applied to the samples. The cameras are calibrated via a high contrast dot pattern of known diameter and spacing. In these set-ups, it was a 9×9 grid of points with a separation of 10 mm. Once calibrated, the system is ready to photograph the composite beam and determine deflection as a function of time. Reference images of the beams were initially taken after the samples were painted. Subsequent images were taken before starting each testing cycle. These images were contrasted against images taken over the hour observation time to determine the deflection as the sample cooled. Images are captured via VIC Snap 2009 and processed via VIC-3D 2009 to determine deformations. Figure 1.3 shows the digital image correlation experimental set-up to measure the remaining deformation on the generic UCA specimens.

1.2.3 Environmental Chamber Set-Up

The UCAs were placed in a Sun Systems Model EC12 environmental chamber and was used to regulate the temperature to the desired point above the shape memory polymer glass transition temperature. The temperature was monitored via a thermocouple inside of the chamber and confirmed via a Fluke 561 series infrared thermometer. Beam samples were placed on a Teflon plate within the chamber to allow for full expansion under elevated temperature conditions.

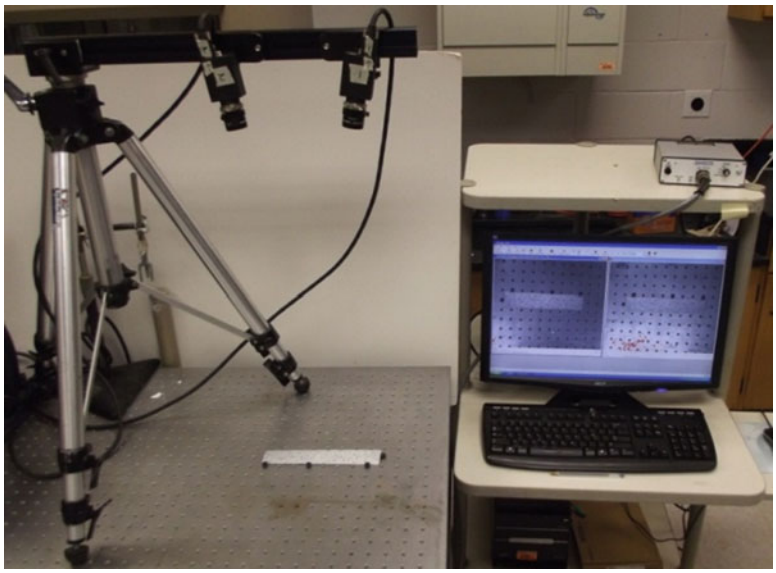

Fig. 1.3 Experimental set-up for DIC analysis of the UCAs

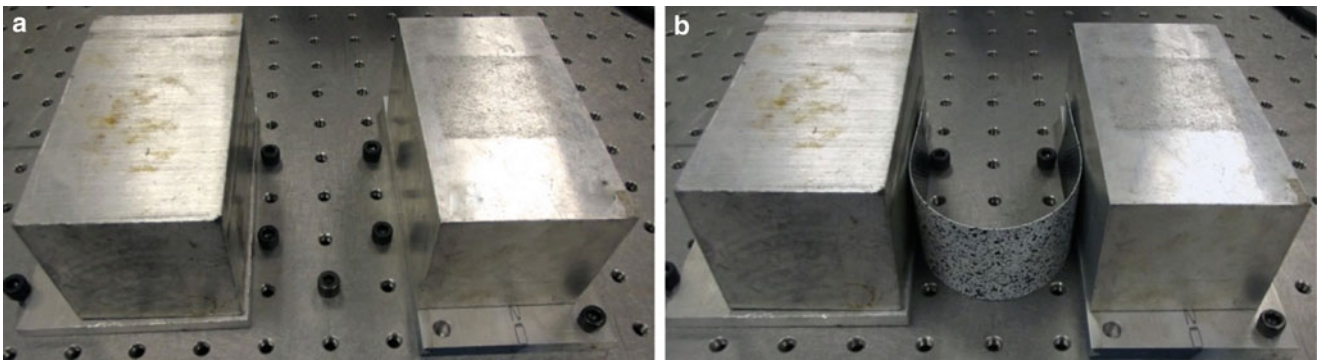

Fig. 1.4 (**a**) Sample container without a sample. (**b**) Sample container holding a curved carbon fiber beam

1.2.4 UCA Sample Holder Set-Up

Once samples were removed from the environmental chamber they were folded into a U-shaped configuration as shown in Fig. 1.4, and stored in a tabletop retainer to ensure equivalent loading conditions for all actuators. This apparatus consisted of five 1/4-20 bolts in a U configuration secured to the table in order to constrain the samples from folding inwardly, and two metal blocks spaced 60 mm apart to constrain the samples in the outward direction.

1.2.5 Procedure to Measure UCA Recoverability

Step-by-Step Procedure to Measure Shape Recovery of the UCA Using DIC

The procedure for measuring the out-of-plane residual deformation with DIC after a temperature cycle is enumerated below.

Step 1. After applying a speckle pattern to the sample take an initial (reference) image of the UCA using the DIC set-up.
Step 2. Place the undeformed UCA in the environmental chamber for 1 h at 85 °C.
Step 3. Bend the UCA beam into a U-shaped configuration and place it within the holder to cool for 1 h in the stored configuration.
Step 4. Return the sample to the environmental chamber set to 85 °C and allow the beam to hold for 1 h at temperature.
Step 5. Remove UCA from the oven to start recovery to original position.
Step 6. Monitor via DIC while the UCA cools to room temperature.

1.3 Unimorph Composite Actuator Results

Out-of-plane deflection (w) was the main focus of the UCA experiments. The goal was a beam with minimal residual deformation that when stored would hold the desired shape. Initial samples consisted of 200 mm long by 38 mm wide flat (zero curvature) and 63.5 mm radius of curvature carbon fiber samples. These samples consisted of a 12.7 mm wide and 1.6 mm thickness strip of shape memory polymer adhered via Araldite 2011 epoxy to the center of the carbon fiber beam. Figure 1.5 shows a mock-up of these variables on a concave curved carbon fiber beam. Figure 1.6 shows a schematic of the flat concave, and convex actuators used for testing.

Post-processing of the DIC data was required to properly determine the deflection for each UCA over time. Post-processing was done by extracting the XYZ coordinates and UVW displacements for the centerline of each sample at the desired timestamp. Next the data are extracted to an Excel file, the deformation (W) data sorted by timestamp, and shifted to the desired coordinate system via MATLAB. Once in the desired X–Z plane, the data are rotated to eliminate rigid body motion making sure to rotate the sample in the X or lengthwise direction to maintain the correct displacement directions. After rotation the data undergo a final vertical translation to the X-axis ensuring all images can be compared in the same coordinate system. This process is illustrated in Fig. 1.7.

Data for both the flat and concave UCA samples were collected in 2 min intervals for the entirety of the 30 min cool down time. The centerline shape was measured for the reference (before any temperature cycle) and at various times after the temperature cycle. To obtain the deformation the reference shape was subtracted from the shape after the temperature cycle. In order to properly control for any manufacturing defects, only the deflection from the original shape is covered in the subsequent results. Table 1.1 shows the maximum out-of-plane deflection for both the flat and concave samples while Figs. 1.8, 1.9, 1.10, and 1.11 show the centerline deformation along the longitudinal direction for both samples through

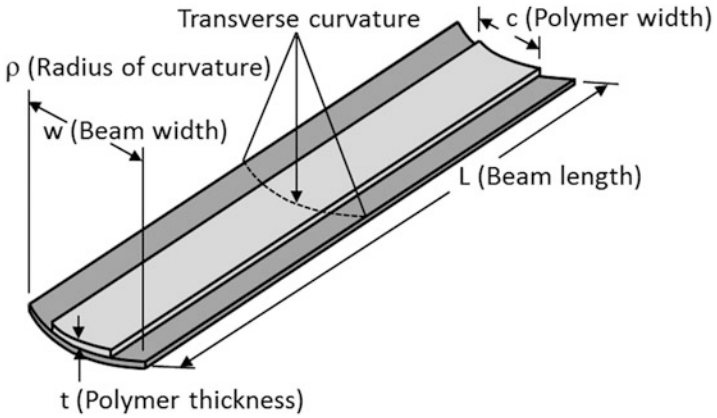

Fig. 1.5 Illustration of the variables present on a UCA

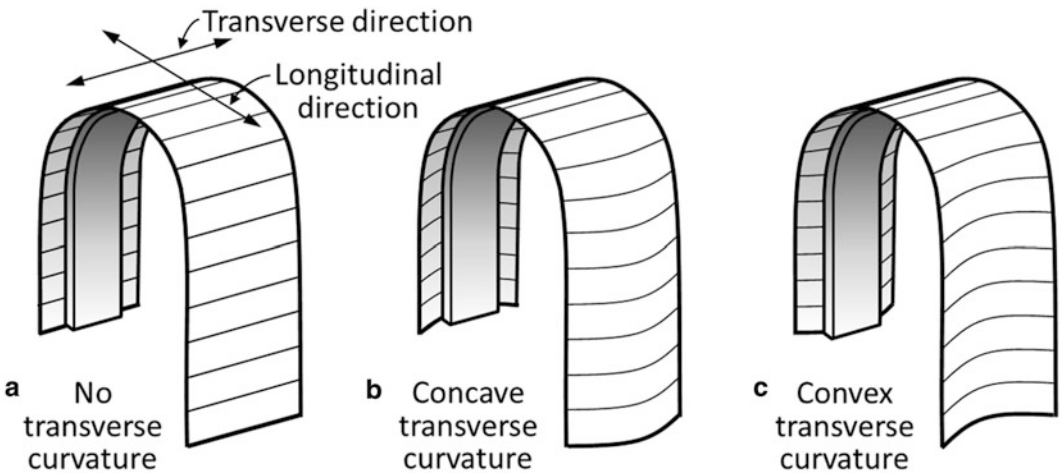

Fig. 1.6 Comparison of a UCA (**a**) without curvature (flat composite), (**b**) with concave transverse curvature, and (**c**) a UCA with convex transverse curvature

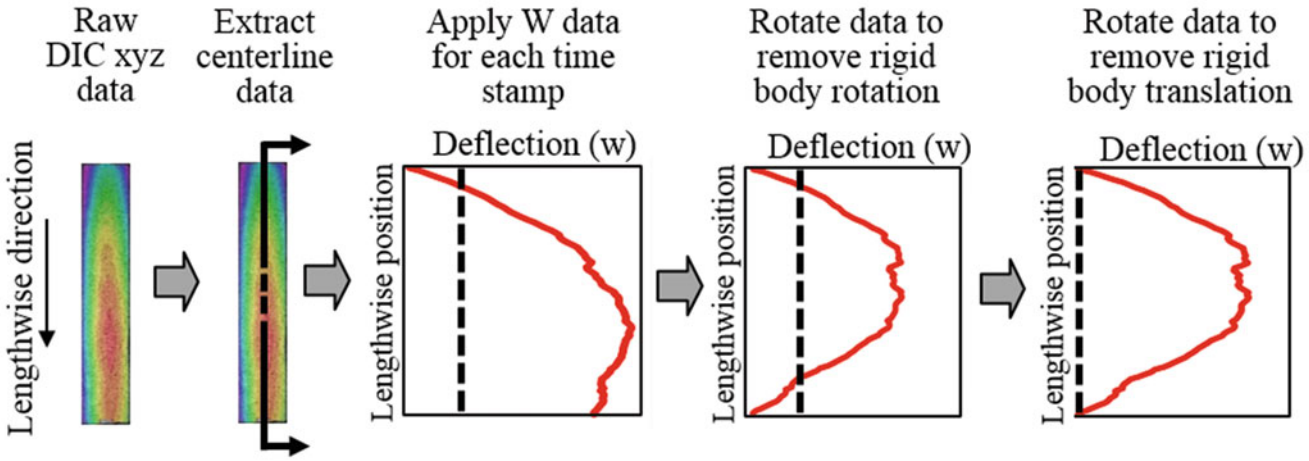

Fig. 1.7 Illustration of the process of converting the DIC data to the desired coordinate system and removing rigid body motion

Table 1.1 Maximum deflections for the UCA samples at each marked time

Time (min)	Max deflection concave sample (recovered-reference) (mm)	Max deflection flat sample (recovered-reference) (mm)
Reference	0.00	0.00
2	0.28	5.89
4	0.34	9.80
6	0.35	11.4
8	0.35	12.0
10	0.35	12.1
20	0.31	12.3
30	0.30	12.7

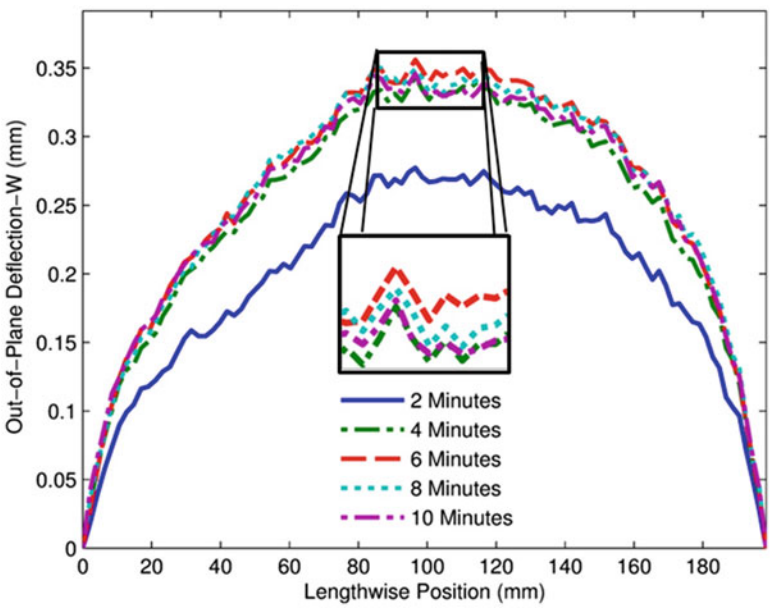

Fig. 1.8 Lengthwise versus out-of-plane deflection for the first 10 min of the 63.5 mm concave UCA cooling cycle

30 min. The data clearly show that the concave sample has significantly less residual deformation than the flat sample over the 30 min trial. The concave sample has a maximum variation from the original sample of only 0.35 mm while the flat sample has a maximum difference of 12.7 mm. The graphs show that the concave UCA reaches a peak deflection at approximately 6 min then relaxes a distance of 60 μm by the 30 min mark. The flat UCA does not reach equilibrium in

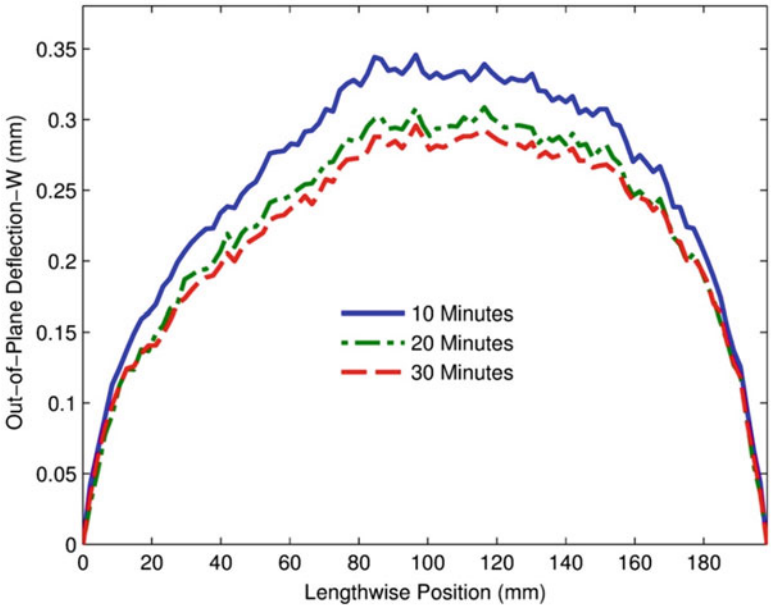

Fig. 1.9 Lengthwise position versus out-of-plane deflection for times 10–30 min of the 63.5 mm concave UCA cooling cycle

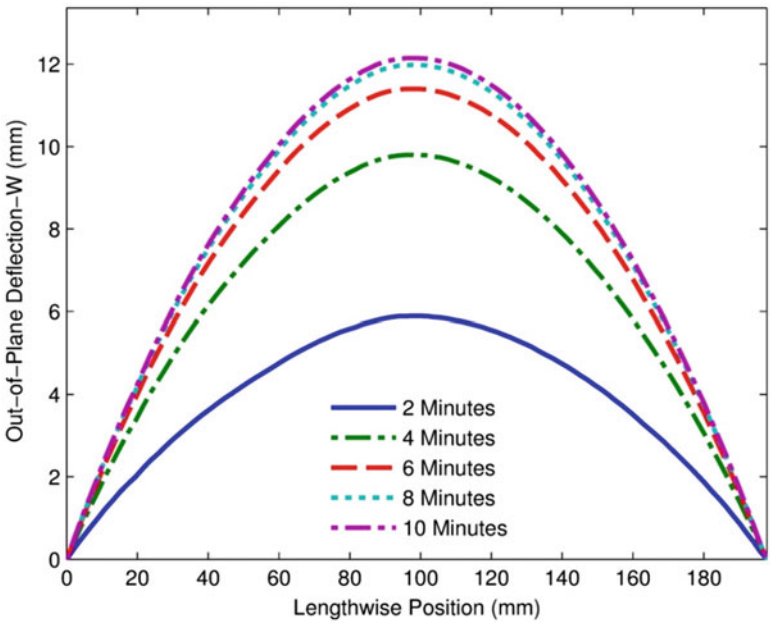

Fig. 1.10 Lengthwise position versus out-of-plane deflection for the first 10 min of the flat UCA cooling cycle

30 min as it continues to deflect until the 30 min mark. However, the data show that a majority of the deformation has already occurred after 6 min which was also true of the concave sample.

The preliminary test clearly shows that the concept of applying concave transverse curvature to a unimorph substrate substantially improves shape recovery. As such in order to explore further this concept, an additional curved UCA was created but instead of the conventional concave orientation (saddle configuration) it was created with convex orientation (trough configuration). The convex sample was constructed to determine the effect on the residual deformation in an alternate orientation. An example of a convex sample was shown previously in Fig. 1.6. The convex set of samples was monitored via DIC for 30 min during the cool down like the previously tested samples. Table 1.2 shows the maximum out-of-plane deviation with respect to time for the convex sample versus the original concave sample. The data show that while the original concave sample had more initial deformation the convex sample has the larger change in residual deflection. As stated previously, the concave sample deflects only 0.35 mm whereas the convex sample deflects 1.29 mm in the same time period. The convex sample behaves similarly to the concave sample with respect to relaxation. Both samples reach maximum deflection at approximately 6 min and decrease in deflection to some extent up to the 30 min. Figures 1.12 and 1.13

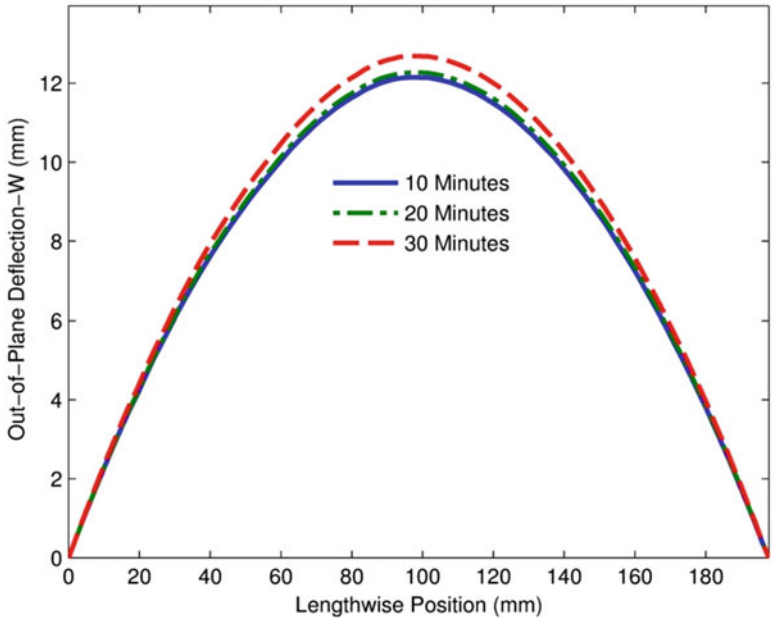

Fig. 1.11 Lengthwise position versus out-of-plane deflection for times 10–30 min of the flat UCA cooling cycle

Table 1.2 Maximum deflections for the UCA samples at each marked time

Time (min)	Max deflection concave sample (recovered-reference) (mm)	Max deflection convex sample (recovered-reference) (mm)
Reference	0.00	0.00
2	0.28	0.86
4	0.34	1.19
6	0.35	1.29
8	0.35	1.29
10	0.35	1.29
20	0.31	1.20
30	0.30	1.13

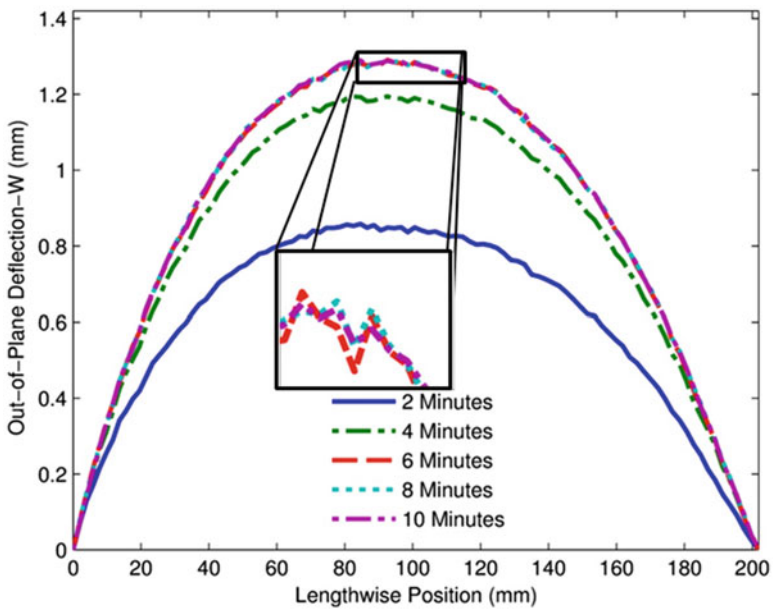

Fig. 1.12 Lengthwise position versus out-of-plane deflection for the first 10 min of the convex UCA cooling cycle

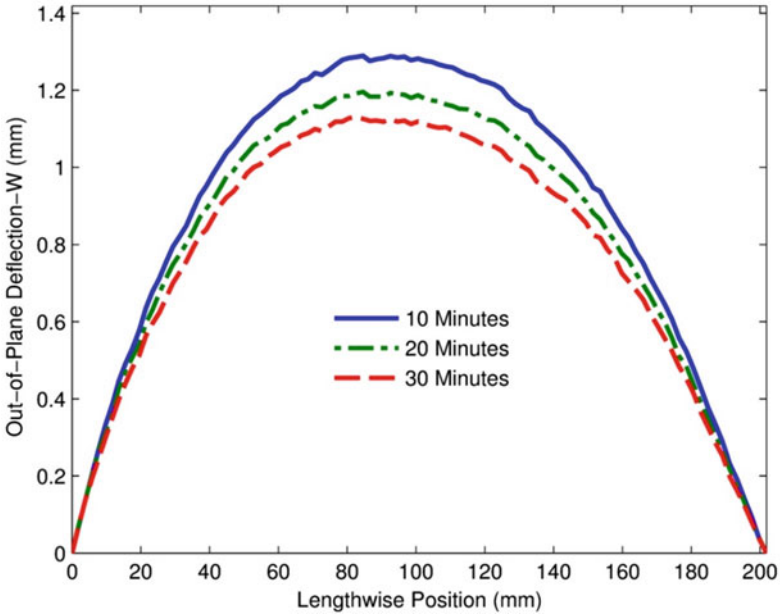

Fig. 1.13 Lengthwise position versus out-of-plane deflection for times 10–30 min of the convex UCA cooling cycle

Table 1.3 Repeatability test data for the concave curved UCA sample

Time (min)	Test 1 position (mm)	Test 2 position (mm)	Test 3 position (mm)	Test 4 position (mm)	Standard deviation (mm)	Coefficient of variation (%)
6	1.93	1.95	1.91	1.93	1.63E−2	0.85
60	1.81	1.80	1.78	1.81	1.41E−2	0.78

support these findings and show the centerline deformations for the convex sample. The results indicate the original concave configuration should be used for any further testing due to the minimal deflections seen under comparable conditions.

A final series of testing was done on a new concave curved sample to determine the repeatability of testing and any residual deformation as additional deflection cycles were performed on the UCA. A series of four consecutive tests were conducted and compared at the maximum out-of-plane position (Z + W) time of 6 min as well as at the end of the data collection period. Table 1.3 shows the data range was only 40 μm at 6 min and 30 μm at 60 min. Both values that are well within an acceptable range for repeatability.

1.4 Conclusion

A series of tests were conducted on carbon fiber and shape memory polymer composite actuators to determine the effect of radius of curvature on the residual deformation. Digital image correlation was employed to find the out-of-plane deformation and allowed for the study of the recovery behavior of these unimorph composite actuators. In the experiments conducted a unimorph composite actuator with a 63.5 mm concave transverse curvature was able to reduce residual deformation by two orders of magnitude compared to a flat unimorph composite actuator keeping all other variables constant. A unimorph with convex transverse curvature was only able to reduce residual deformation by one order of magnitude making a concave actuator the best option for future use. Unimorph composite actuators display repeatable actuation and storage cycles as they do not increase residual deformation with increasing number of cycles. These discoveries can facilitate the expanded use of shape memory polymers on a reconfigurable folding wing micro air vehicles as well as various other applications.

Future research will continue to develop the design space presented in this paper. Unimorph composite actuators with varying transverse curvature polymer thickness, substrate width, and polymer width will all be evaluated to determine the correlation between each variable and residual deformation.

References

1. Otsuka K, Wayman CM (eds) (1998) Shape memory materials, 1st edn. Cambridge University Press, Cambridge, p 284
2. Lacroix BW, Ifju PG (2012) Utilization and performance enhancements of multiple piezoelectric actuators on micro air vehicles. In: AIAA aerospace sciences meeting, pp 1–14
3. Lacroix BW, Ifju PG (2013) Macro fiber composites and substrate materials for MAV wing morphing. In: Society for experimental mechanics, pp 1–13
4. Yakacki CM, Shandas R, Lanning C, Rech B, Eckstein A, Gall K (2007) Unconstrained recovery characterization of shape-memory polymer networks for cardiovascular applications. Biomaterials 28(14):2255–2263
5. Thill C, Etches J, Bond I, Potter K, Weaver P (2008) Morphing skins. Aeronaut J 112(3216):1–23
6. Fulcher JT, Karaca HE, Tandon GP, Foster DC, Lu YC (2011) Multiscale characterization of water-, oil-, and UV-conditioned shape-memory polymer under compression. In: Mechanics of time-dependent materials and processes in conventional and multifunctional materials, pp 97–103
7. Fulcher JT, Karaca HE, Tandon GP, Lu YC (2012) Thermomechanical and shape memory properties of thermosetting shape memory polymer under compressive loadings. J Appl Polym Sci
8. Fulcher JT (2011) Mechanical characterizations of environmentally conditioned shape memory polymers for reconfigurable aerospace structures. University of Kentucky
9. Nahid MNH, Wahab MA, Lian K (2011) Degradation of shape memory polymer due to water and diesel fuels. In: Mechanics of time-dependent materials and processes in conventional and multifunctional materials, pp 37–48
10. McClung AJW, Tandon GP, Goecke KE, Baur JW (2011) Non-contact technique for characterizing full-field surface deformation of shape memory polymers at elevated and room temperatures. Polym Test 30(1):140–149
11. McClung AJW, Ruggles-Wrenn MB (2009) Strain rate dependence and short-term relaxation behavior of a thermoset polymer at elevated temperature: experiment and modeling. J Press Vessel Technol 131(3):031405
12. McClung AJW, Tandon GP, Baur JW (2011) Fatigue cycling of shape memory polymer resin. In: Mechanics of time-dependent materials and processes in conventional and multifunctional materials, vol 3, pp 119–127
13. McClung AJW, Tandon GP, Baur JW (2011) Strain rate- and temperature-dependent tensile properties of an epoxy-based, thermosetting, shape memory polymer (Veriflex-E). Mech Time-Dependent Mater 16(2):205–221
14. McClung AJW, Tandon GP, Baur JW (2011) Deformation rate-, hold time-, and cycle-dependent shape-memory performance of Veriflex-E resin. Mech Time-Dependent Mater 17(1):39–52
15. Liu Y, Gall K, Dunn ML, Greenberg AR, Diani J (2006) Thermomechanics of shape memory polymers: uniaxial experiments and constitutive modeling. Int J Plast 22(2):279–313
16. Atli B, Gandhi F, Karst G (2008) Thermomechanical characterization of shape memory polymers. J Intell Mater Syst Struct 20(1):87–95
17. Carrell J, Tate D, Wang S, Zhang H-C (2011) Shape memory polymer snap-fits for active disassembly. J Clean Prod 19(17–18):2066–2074
18. Lan X, Liu Y, Lv H, Wang X, Leng J, Du S (2009) Fiber reinforced shape-memory polymer composite and its application in a deployable hinge. Smart Mater Struct 18(2):024002
19. Joo J, Smyers B, Beblo R, Reich G, Force A (2011) Load-bearing multi-functional structure with direct thermal harvesting for thermally activated reconfigurable wing design. In: International conference on composite materials, pp 1–6
20. Leng J, Lu H, Liu Y, Huang WM, Du S (2009) Shape-memory polymers — a class of novel smart materials. MRD Bull 34(11):848–855
21. Monkman G (2000) Advances in shape memory polymer actuation. Mechatronics 10(4–5):489–498
22. Schmidt C, Neuking K, Eggeler G (2008) Functional fatigue of shape memory polymers. Adv Eng Mater 10(10):922–927
23. Gall K, Mikulas M, Munshi N a, Beavers F, Tupper M (2000) Carbon fiber reinforced shape memory polymer composites. J Intell Mater Syst Struct 11(11):877–886
24. Liu C, Qin H, Mather PT (2007) Review of progress in shape-memory polymers. J Mater Chem 17(16):1543
25. Beloshenko V a, Varyukhin VN, Voznyak YV (2005) The shape memory effect in polymers. Russ Chem Rev 74(3):265–283
26. Vaia R, Baur J (2008) Materials science: adaptive composites. Science 319(5862):420–421
27. Cantrell JT, Lacroix BW, Ifju PG (2013) Passive roll compensation on micro air vehicles with perimeter reinforced membrane wings. Int J Micro Air Veh 5(3):163–177
28. Ifju PG, Jenkins DA, Waszak MR, Ettinger S, Lian Y, Shyy W (2002) Flexible-wing-based micro air vehicles, pp 1–13
29. Shyy W, Ifju P, Viieru D (2005) Membrane wing-based micro air vehicles. Appl Mech Rev 58(4):283
30. Stanford BK (2008) Aeroelastic analysis and optimization of membrane micro air vehicle wings. University of Florida
31. Albertani R (2005) Experimental aerodynamic and static elastic deformation characterization of low aspect ratio flexible fixed wings applied to micro aerial vehicles. University of Florida
32. Ifju P, Lee K, Albertani R, Mitryk SJ, Mary L, Boria FJ, Abd (2008) Bendable wing for micro air vehicle. 7,331,5462008
33. Sutton MA, Turner JL, Bruck HA, Chae TA (1991) Full-field representation of discretely sampled surface deformation for displacement and strain analysis. Exp Mech 31:168–177
34. Sutton MA (2008) Springer handbook of experimental solid mechanics. Department of Mechanical Engineering, The Johns Hopkins University, Baltimore, pp 565–600

Chapter 2
Yield Criterion for Polymeric Matrix Under Static and Dynamic Loading

B.T. Werner and I.M. Daniel

Abstract A polymeric matrix (3501-6) used in composite materials was characterized under multi-axial quasi-static and dynamic loading at varying strain rates. Tests were conducted under uniaxial compression, tension, pure shear and combinations of compression and shear. Quasi-static and intermediate strain rate tests were conducted in a servo-hydraulic testing machine. High strain rate tests were conducted using a split Hopkinson Pressure Bar system built for the purpose. This SHPB system was made of glass/epoxy composite (Garolite) bars having an impedance matching the test polymer closer than metals. The typical stress–strain behavior exhibits a linear elastic region up to a yields point, a nonlinear elastoplastic region up to an initial peak or critical stress, followed by a strain softening region up to a local minimum and finally, a strain hardening region up to ultimate failure. It was observed that under multi-axial loading, yielding is governed by one characteristic property, the yield strain under uniaxial tension. Furthermore, it was found that the yield point varied linearly with the logarithm of strain rate. A general three-dimensional elasto-viscoplastic model was formulated in strain space expressed in terms of an effective strain and its yield point. A unified yield criterion was proposed to describe the onset of yielding under any state of stress and at any strain rate.

Keywords Polymer-matrix • Multi-axial testing • Elastic–plastic behavior • Yield criteria • Strain rate effects

2.1 Introduction

Recent and ongoing research in fiber reinforced polymer composites has dealt with material characterization, constitutive behavior and failure prediction. The process of fabrication, testing and modeling of these composites is costly and time consuming and impedes the introduction of new materials. To facilitate and accelerate the process of introducing and evaluating new composite materials, it is important to develop/establish comprehensive and effective methods and procedures of constitutive characterization and modeling of structural laminates based on the properties of the constituent materials, e.g., fibers, polymers and the basic building block of the composite structure, the single ply or lamina.

Lamina characterization and modeling under multi-axial states of stress has shown that there are significant inelastic, nonlinear, viscoelastic and rate effects on the matrix dominated constitutive and failure behavior of these materials [1–3]. In the case of carbon/epoxy composites for example, the fiber itself shows little nonlinear behavior and no rate dependence in its mechanical response. This suggests that the matrix is the key element that controls the inelastic and nonlinear behavior of the composite and that its characterization and modeling are very important. Since the polymer matrix is basically isotropic, a much less costly evaluation of a composite can be achieved by characterizing the bulk matrix under multi-axial states of stress at various strain rates.

The constitutive and strain rate behavior of epoxies under various loading conditions has been studied by many researchers including the authors of this paper [4–14]. Some studies describe characterization of the resin at various strain

B.T. Werner
Sandia National Laboratories, Livermore, CA, USA
e-mail: bwerner@sandia.gov

I.M. Daniel (✉)
Northwestern University, Evanston, IL, USA
e-mail: imdaniel@northwestern.edu

H.J. Qi et al. (eds.), *Challenges in Mechanics of Time-Dependent Materials, Volume 2: Proceedings of the 2014 Annual Conference on Experimental and Applied Mechanics*, Conference Proceedings of the Society for Experimental Mechanics Series,
DOI 10.1007/978-3-319-06980-7_2,